Variable Space Vector Modulation for Self-Sensing Magnetic Bearings

Dominik Wimmer, Markus Hutterer, Matthias Hofer, Manfred Schrödl

Technische Universität Wien, Gußhausstraße 25-29, A-1040 Vienna, Austria, dominik.wimmer@tuwien.ac.at

***Abstract*—The subject of this paper is an improvement of a self-sensing control of a three-phase radial magnetic bearing based on the so called INFORM method. The focus of this paper lies on a modification of the space vector modulation to achieve a high position resolution as well as a high actuator dynamic at low DC-link voltage levels. Therefore, certain constraints for the space vector modulation must be fulfilled to allow a self-sensing operation of the bearing. For this reason, different kinds of space vector modulations are designed theoretically as well as proven in experiments on a prototype of a radial magnetic bearing. Finally, the obtained performance of the INFORM method is shown by a linearity measurement and a comparison of the small signal behavior by means of external position sensors.**

I. Introduction

Active magnetic bearings (AMB) are of great significance for the stabilization of levitating rotors. The self-sensing operation of AMBs has been a field of research for many years [1] and provides advantages concerning sensor failure, construction space and production costs of the AMB. In this proposal the so called INFORM (Indirect Flux Detection by Online Reactance Measurement) method is used to determine the rotor position. This method was originally designed for the rotor angle determination of a permanent magnet synchronous motor [2]. At AMBs, the INFORM method is based on a current slope measurement, detecting the inductance change of an eccentric rotor. The first implementation for a self-sensing operation of an AMB was performed with an injection of high frequency voltage pulses to the actuator coils [3], [4]. Therefore, the current controller stops in equidistant time steps and measurement pulses are applied to the coils. This approach has the drawback of a limited bandwidth of the position measurement and an interruption of the current controller. To avoid this circumstance, the required measurement pulse pattern is embedded in the pulse width modulation (PWM) sequence of the current controller. The use of an embedded INFORM pulse pattern, in particular the 3-Active INFORM pattern [5], is the point of origin for the space vector modulation in this work.

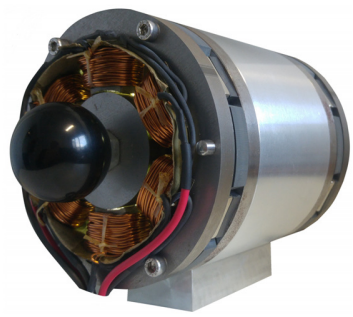

Figure 1: Prototype of a self-sensing homopolar radial magnetic bearing with six poles. The bias flux is realized by the use of permanent magnets (PM).

II. Problem Formulation

Measurements on a prototype of a self-sensing radial AMB (Fig. 1) have shown significant power losses in the bearing in the 3-Active PWM mode. Consequently, the power losses lead to a temperature rise in the bearing, which is undesirable in many applications. Beside the control current, the current ripple of the coils causes significant power losses in the AMB. Hence, the major power losses in the prototype occur in the flux leading paths by means of iron losses in the laminated iron sheets. One possible solution for the reduction of the eddy current losses is the use of soft magnetic composites (SMC), which is described in Hofer et al. [6]. However, SMC materials have drawbacks like a smaller permeability and mechanical limitations [7]. This paper follows an approach, which is independent of the used material. Figure 2(a) shows the power loss of the prototype (Fig. 1) as a function of the DC-link

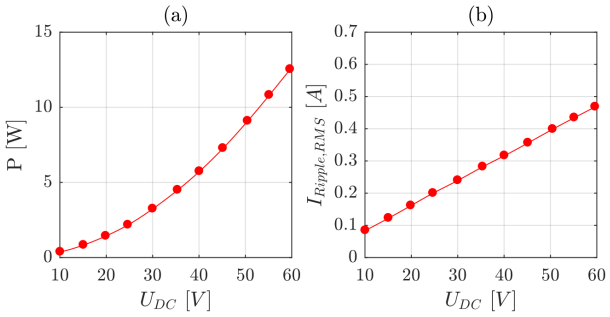

Figure 2: Power losses of the bearing (a) due to the current ripple (b) as a function of the DC-link voltage. (3-Active space vector modulation, f_{PWM} = 20kHz, rotor is levitating at standstill)

voltage U_{DC}. For a fixed switching frequency, it is obvious to decrease U_{DC} for achieving small power losses. On the one hand, a high value of U_{DC} causes a high current ripple (Fig. 2(b)), which provides a high magnitude of the current slope information. On the other hand, the iron losses are increased and therefore undesirable power losses occur in the

flux leading paths. To keep the power losses in the bearing small, a low level of U_{DC} is aspired. This circumstance gives the motivation to enhance the INFORM measurement for dealing with small current slopes. Further, it must be considered that the dynamic of the current controller depends on U_{DC}. Accordingly, the space vector modulation (SVM) enables further degrees of freedom to influence the performance of the bearing. The focus of this paper lies on investigation of different space vector modulations regarding to a high current dynamic as well as a high quality of the position measurement. The design of SVM contains degrees of freedom, which can be used for the development of specific pulse patterns with especially high current dynamics or high quality of the position measurement. Taking this one step further, it is possible to use different kinds of SVM during the operation of the AMB. This leads to the variable SVM and enables the combination of the properties of different modulations.

III. Radial Bearing Setup

The bearing setup of Figure 1 consists of two radial homopolar six pole AMBs as illustrated in Figure 4. Two opposite coils are corresponding to one phase, which enables the use of a conventional three-phase inverter. Figure 3 shows a differential transformer, which is the point of connection between the positive and negative phase of the bearing. By the usage of the measurement transformer in each phase, it is

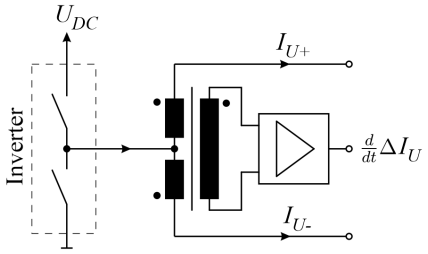

Figure 3: Measurement of the differential current slope signal by means of a differential transformer.

possible to connect the AMB to a three-phase inverter. The transformer output provides the differential current slope signal, which is required for the self-sensing INFORM operation of the bearing. Thus, the rotor position is given by

$$U(t) = L(x,y)\frac{d}{dt}\Delta I(t) \;\rightarrow\; L(x,y) = U(t)\left(\frac{d}{dt}\Delta I(t)\right)^{-1} \quad (1)$$

the position-depending inductance $L(x,y)$ of equation (1) [5].

IV. Space Vector Modulation

Figure 4 shows the symmetrical arrangement of the magnetic poles of the bearing. The spatially distributed arrangement of the poles enables the definition of six fundamental voltage space vectors, which are aligned with the magnetic poles of the bearing. The fundamental space vectors shape a hexagon, which defines the possible modulation range

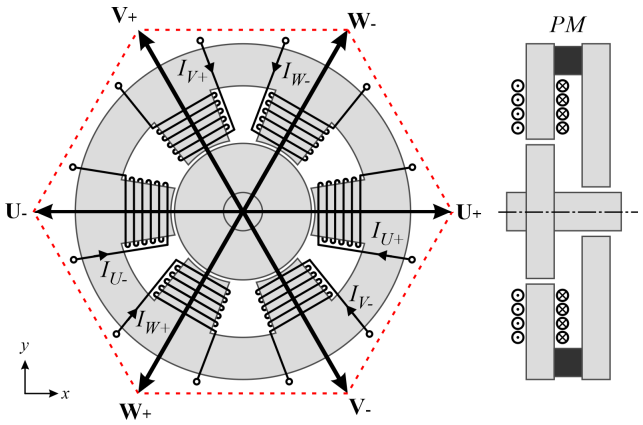

Figure 4: Cross section of the six pole homopolar radial AMB. The fundamental space vectors **U**+, **U**-, **V**+, **V**-, **W**+, **W**- are aligned with the poles.

of voltage space vectors. Each point in this hexagon can be reached by a linear combination of the fundamental space vectors (**U**+, **U**-, **V**+, **V**-, **W**+, **W**-) and the zero space vectors (**Z**+, **Z**-). The zero space vector occurs if either all high-side or low-side switches of the three-phase inverter are closed. The degree of freedom in the composition of the linear combination of the fundamental space vectors is used to design different kinds of SVM.

A. Design rules for SVM

The design criteria of the SVM are achieving a good quality of the position measurement and a high current controller bandwidth. Therefore, the design of the SVM underlies certain restrictions to allow a self-sensing operation of the magnetic bearing:

- **INFORM method:** Theoretically, the current ripple due to a single voltage pulse contains the whole information of the rotor position. Due to the fact that asymmetries appear in the real system (caused by mechanical, electrical or magnetic deviations), it is beneficial to use the current slope information from independent voltage pulses. Furthermore, the voltage pulses must have a minimal pulse duration t_{INF} (relative to the PWM period), which is given by the settling time of the current slope measurement. The duration is defined by the decay of the eddy currents (approx. 7 µs), which causes a distortion of the current slope signal.

- **Modulation amplitude:** The modulation amplitude defines the maximum length of a space vector. High modulation amplitudes allow a high dynamic of the current control. For a symmetrical, angle independent, operation of the current controller, it is beneficial to limit the modulation amplitude to the in-circle of the possible modulation area. The theoretical maximum for a system with six poles is ≈ 0.866.

- **Inverter:** Short pulse lengths could cause problems in semiconductor switches. Hence, the specified recovery time of the switches must be considered in the PWM pattern. Furthermore, the pulse pattern has to provide a

switching action in each phase to ensure a proper operation of a potential charge pump of the gate driver.

The design procedure of the SVM is based on representation of the voltage space vector **P**, which is specified by the superior current controller. Hence, the space vector **P** is given by equation (2) by means of the fundamental space vectors.

$$\mathbf{P} = c_{U_+}\mathbf{U}_+ + c_{V_+}\mathbf{V}_+ + c_{W_+}\mathbf{W}_+ + c_{Z_+}\mathbf{Z}_+ \\ c_{U\_}\mathbf{U}_- + c_{V\_}\mathbf{V}_- + c_{W\_}\mathbf{W}_- + c_{Z\_}\mathbf{Z}_- \quad (2)$$

Therefore, the coefficients c_{U_+}, c_{U_-}, c_{V_+}, c_{V_-}, c_{W_+}, c_{W_-}, c_{Z_+}, $c_{Z\_}$ define the length of the corresponding space vector. The following introduced variants of SVM differ substantially in the number of the active space vectors within one PWM period. In this context, "active" refers to the fundamental space vectors with an amplitude unlike zero.

B. 6-Active SVM

The 6-Active SVM uses all fundamental space vectors (except the zero space vectors) for the formation of **P**. Figure 5 shows the possible symmetrical modulation area $\|\mathbf{P}\|_2$, which is given by the minimum and maximum symmetrical

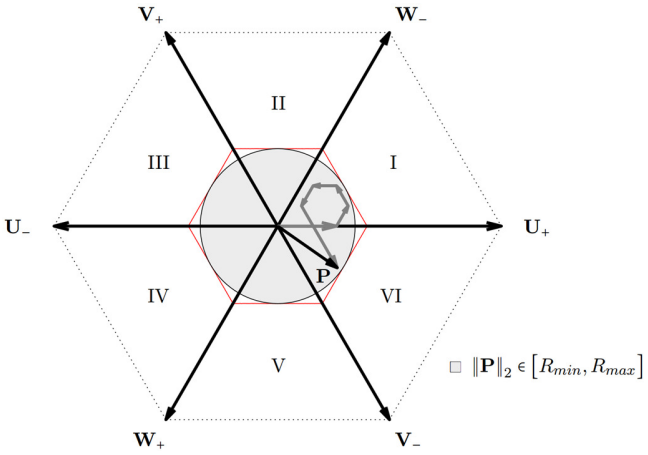

Figure 5: 6-Active SVM: The space vector **P** is formed by the fundamental space vectors, except the the zero space vectors **Z**+, **Z**-.

modulation amplitude (R_{min}, R_{max}). The 6-Active SVM allows six independent current slope measurements within a PWM period. For this reason, the 6-Active SVM is well suitable for the self-sensing method. However, this kind of modulation has the drawback of a very limited modulation amplitude R_{max}. The impact of the small value of R_{max} is caused by the minimal pulse width t_{INF} by means of equ. (3).

$$R_{max} = \frac{\sqrt{3}}{2}(1 - 6\,t_{INF}),\ t_{INF} < \frac{1}{6} \\ R_{min} = 0 \quad (3)$$

For achieving a higher value of R_{max}, the number of space vectors is reduced in the following considerations.

C. 3-Active LDR SVM

In contrast to the 6-Active SVM, the 3-Active Low Dynamic Range (LDR) SVM uses either three positive (**U**+, **V**+, **W**+) or three negative fundamental space vectors (**U**-, **V**-, **W**-). Figure 6 shows a 3-Active LDR SVM with a linear combination of **U**+, **V**+, **W**+. Due to the use of only three fundamental space vectors, the maximum modulation amplitude is limited to $1/2$, but has a

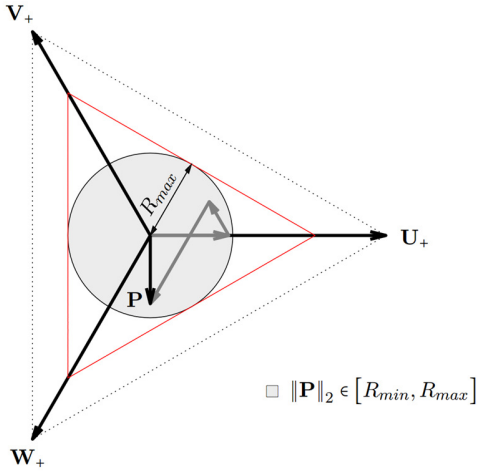

Figure 6: 3-Active LDR SVM: The space vector **P** is formed by the positive fundamental space vectors (**U**+, **V**+, **W**+).

$$R_{max} = \frac{1}{2}(1 - 3\,t_{INF}),\ t_{INF} < \frac{1}{3} \\ R_{min} = 0 \quad (4)$$

smaller drop of R_{max} by an increase of t_{INF} (equ. (4)).

D. 4-Active SVM

The 4-Active SVM is based on the 3-Active LDR SVM, but enhances the modulation amplitude by means of an additional fundamental space vector (Fig. 7), which is located next to the

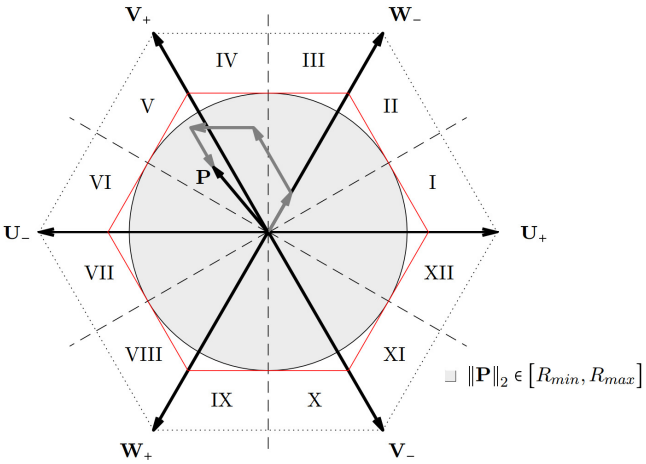

Figure 7: 4-Active SVM: The space vector **P** is formed by the negative (**U**-, **V**-, **W**-) fundamental space vectors and **V**+ for an enhancement of the modulation amplitude.

desired space vector **P**. Furthermore, the use of positive (**U**+, **V**+, **W**+) or negative (**U**-, **V**-, **W**-) fundamental space vectors is dependent of the sector (I-XII) to obtain a high value of R_{max}.

$$R_{max} = \frac{\sqrt{3}}{2}(1 - 3\,t_{INF}),\ \ t_{INF} < \frac{1}{5} \qquad (5)$$
$$R_{min} = 0$$

In contrast to the 3-Active LDR SVM, the maximum modulation amplitude is enhanced by a factor of $\sqrt{3}$ (equ. (5)).

E. 3-Active HDR SVM

The 3-Active High Dynamic Range (HDR) SVM is designed for a maximum modulation amplitude using three

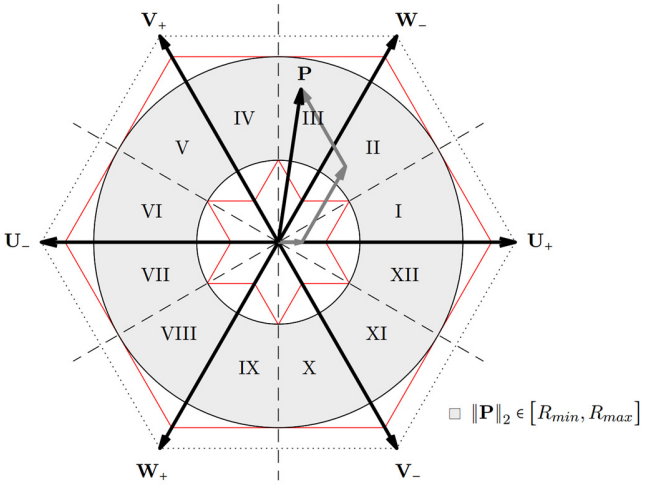

Figure 8: 3-Active HDR SVM: The desired space vector **P** is built with three fundamental space vectors (from a separate phase) and one zero space vector.

active fundamental space vectors and one zero space vector (**Z**+, **Z**-). The desired space vector **P** is mainly formed by the two adjoining fundamental space vectors (**V**+, **W**- in Fig. 8). In order to get a current slope information by a voltage space vector from all space axis, the remaining fundamental space vector (**U**+ in Fig. 8) is added with the minimum length t_{INF}. A zero space vector fills the remaining time of the pulse pattern and ensures the required switching action for a proper operation of an existing charge pump of the gate driver. Equation (6) shows the possible modulation range

$$R_{max} = \frac{\sqrt{3}}{2}(1 - t_{INF}),\ \ t_{INF} < \frac{1}{5} \qquad (6)$$
$$R_{min} = 2\sqrt{3}\,t_{INF}$$

for a symmetrical operation.

F. Combination of the SVMs

The design of the SVMs shows, that each SVM has individual characteristics concerning the modulation amplitude and the usability for self-sensing operation. For an optimal operation of the bearing, it is possible to combine the properties

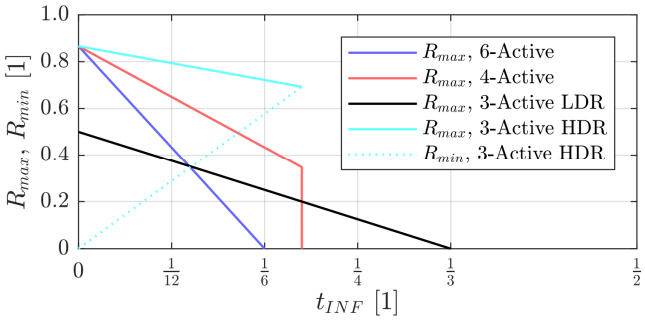

Figure 9: Comparison of the symmetrical modulation amplitude.

of different SVMs. Figure 9 shows a comparison of the symmetrical modulation amplitudes as a function of t_{INF}. The 3-Active HDR has the mannerism of a lower boundary R_{min} of the modulation amplitude. It is obvious, that a low value of

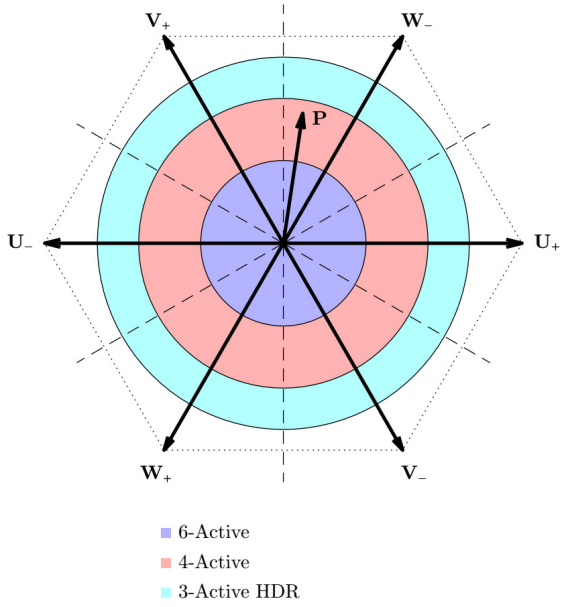

Figure 10: Combination of different SVMs during operation for achieving a high modulation area and a good performance of the self-sensing position measurement. ($t_{INF} = 0.1$)

t_{INF} leads to a high maximum modulation amplitude. The 3-Active LDR can operate up to $t_{INF} < 1/3$, which can be advantageous for applications with a high switching frequency. Concerning the performance of the self-sensing operation, each fundamental space vector gives additional information for the rotor position. Figure 10 shows a combination of multiple SVMs for $t_{INF} = 0.1$. The desired space vector **P** is always built of the SVM, which provides the maximum number fundamental space vectors within a PWM period. To avoid nonessential switching between different SVMs, a hysteresis can be defined by means of an overlapping modulation area.

V. MEASUREMENTS AND RESULTS

The following measurements show a comparison of the behavior of the designed SVMs, regarding to power losses, dynamic of the current controller as well as the quality of the

self-sensing position measurement. The measurements are performed on the prototype presented in Figure 1 with the test setup of Figure 11 respectively. The homopolar radial

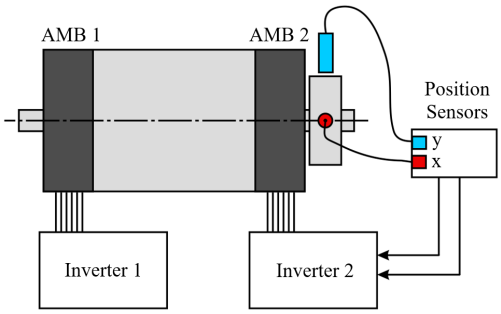

Figure 11: Symbolic arrangement of the test setup with external position sensors according to Figure 1.

magnetic bearings are controlled by separate inverters. Basically, a decoupled control of the rotor gives many degrees of freedom for advanced control [8]. However, a simple decentralized PIDT1 position controller provides sufficient performance for the following considerations.

A. *Power losses of the SVMs*

The initial aim was to decrease the power losses in the bearing by a reduction of the DC-link voltage. Figure 12(a) shows a comparison of the power losses in the bearing for

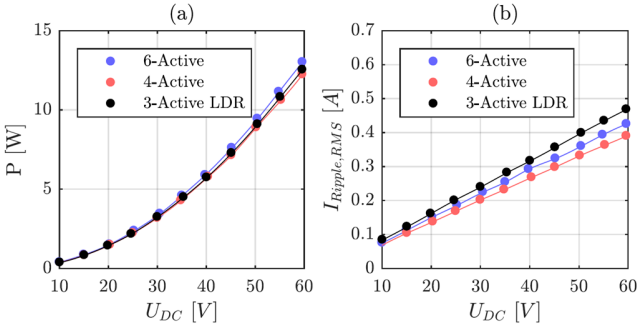

Figure 12: Comparison of the power losses in the bearing (a) due to the current ripple (b) as a function of the DC-link voltage. (f_{PWM} = 20kHz, rotor is levitating at standstill)

different SVMs at 20kHz switching frequency. There is no significant difference between the SVMs, which allows the use of different SVMs.

B. *Dynamic of the current controller*

The maximum modulation amplitude R_{max} of the particular SVM has a significant impact on the dynamic of the current controller. Figure 13(a) shows a comparison of the dynamic of the current controller by means of the step response. Due to the fact that the 3-Active HDR SVM is not able to represent a modulation amplitude smaller than R_{min} (Fig. 9), it is combined with the 4-Active SVM to obtain a

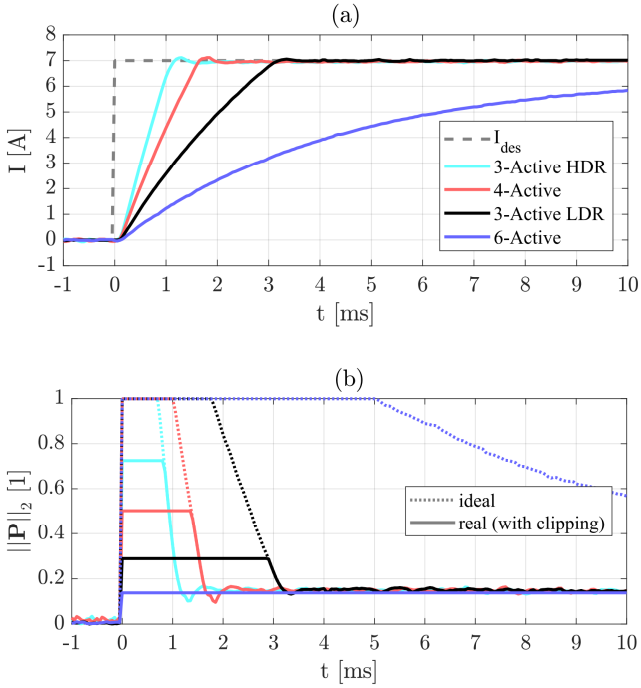

Figure 13: Step response of the current controller (a) with the corresponding magnitude of the desired voltage space vector **P** (b). (f_{PWM} = 20kHz, U_{DC} = 12V, t_{INF} = 0.14)

steady state without oscillation. Figure 13(b) indicates the amplitude of the desired voltage space vector **P**, which corresponds to the step response. It can be seen, that the 3-Active HDR SVM has the highest modulation amplitude. Thus, the controller is only saturated for a short period of time at R_{max}. Concerning Figure 2(b), the 6-Active SVM is not able to inject the desired current of 7A to the coil. The reason is caused by the coil resistance and the connector cable. In this case, the 6-Active modulation can only be used for small currents and shows the use case for switching to a SVM with a higher modulation amplitude.

C. *Noise of the self-sensing INFORM method*

The noise of the self-sensing method is of great significance for a precise control of the bearing. Figure 14(a)

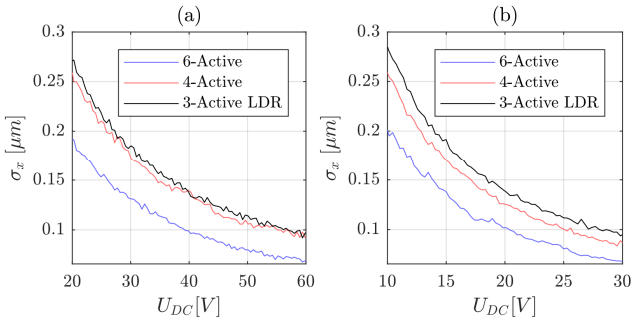

Figure 14: Comparison of the noise of the INFORM-position measurement (a). Reduction of the noise at low levels of U_{DC} by an adaption of the analog circuit (b). (f_{PWM} = 20kHz, rotor fixed in the center of the bearing, standard deviation σ_x over 3000 samples of the x-position at each point of U_{DC})

shows a comparison of the noise of the different SVMs with U_{DC} in the range of 20V to 60V. The 6-Active SVM has the lowest noise level, which is caused by the high number of space vectors. Basically, the noise level increases proportional to $\propto U_{DC}{}^{-1}$. However, it is possible to shift the noise level in a certain range by an adaption of the analog circuit. Therefore, a low noise level can be achieved even at low values of U_{DC}. Thus, Figure 14(b) shows a similar noise characteristic like Figure 14(a) at the half DC-link voltage level (e.g. $\sigma_x < 0.15\mu m$ at 19V) by means of an adaption of the analog circuit.

D. Linearity of the INFORM method

Beside the noise level, the self-sensing method must provide a high linearity for a proper operation of the bearing. The prototype has an air gap of 800µm and the safety bearing allows a radial operational range of 400µm. Figure 15 shows a

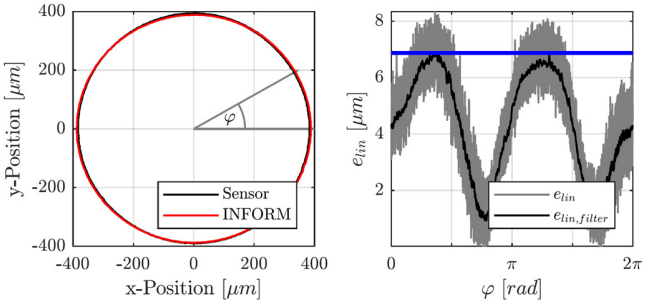

Figure 15: Linearity analysis with external position sensors. The linearity error is given by $e_{lin} = \sqrt{e_x{}^2 + e_y{}^2}$. ($f_{PWM}$ = 20kHz, 6-Active SVM)

linearity analysis of the 6-Active SVM with external position sensors. The overall linearity error e_{lin} is about 7µm, which is already close to the non-linearity of the used reference sensor.

E. Small signal behavior

Finally, a comparison of the small signal behavior shows an example for the accuracy of the self-sensing method. For this purpose, a disturbance is applied to the levitating rotor and the sensor signal is compared to the signal of INFORM

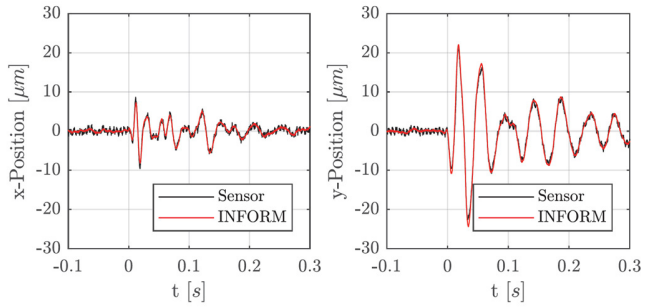

Figure 16: Comparison of the small signal behavior between an external sensor and the INFORM method. A disturbance is applied at $t = 0s$. (f_{PWM} = 20kHz, 6-Active SVM)

method (Fig. 16). Both signals show a consistent behavior, which manifests a precise self-sensing operation.

VI. Conclusion

The focus of this paper lies on a modification of the space vector modulation for three-phase AMBs, regarding to a low power self-sensing operation at low DC-link voltage levels. The design procedure of the space vector modulation shows, that there is a tradeoff between a high modulation amplitude and the usability for the self-sensing operation. Therefore, different SVMs are combined to merge the advantageous properties of the respective SVMs. Hence, the SVM method is switched during the operation of the bearing to achieve a maximum position information for a certain dynamic requirement. Measurements on a prototype show, that the power losses in the bearing are almost independent of the used SVM, which allows a power-neutral switchover of the SVM. Experimental results represent the individual characteristics of the SVMs regarding to dynamic and the noise of the self-sensing position measurement. Moreover, a linearity measurement confirms the accuracy of the self-sensing method. Summarized, it was possible to reduce the DC-link voltage of the prototype by the factor of 2.5 without performance degradations, which results in about 6 times less power losses due to the current ripple.

Further investigations will be done in the switchover characteristics between different space vector modulations, especially with respect to the robustness of the control of the system. In addition, saturation effects of the flux leading paths will be considered regarding to nonlinearities of the self-sensing operation of the AMB.

References

[1] G. Schweitzer, E. H. Maslen, "Theory, Design, and Application to Rotation Machinery", In: *Magnetic Bearings*, Springer Verlag, 2009, pp. 127–145

[2] M. Schrödl, "Sensorless control of permanent-magnet synchronous machines at arbitrary operating points using a modified INFORM flux model", *ETEP* Vo. 3, no 4. July/August 1993

[3] M. Hofer, M. Hutterer, T. Nenning, M. Schrödl, "Improved Sensorless Control of a Modular Three Phase Radial Active Magnetic Bearing", *ISMB14, 14th International Symposium on Magnetic Bearings*, Linz, Austria, August 11-14, 2014

[4] M. Hofer, E. Schmidt, M. Schrödl, "Design of a Three Phase Permanent Magnet Biased Radial Active Magnetic Bearing Regarding a Position Sensorless Control", *Applied Power Electronics Conference and Exposition*, 2009. APEC 2009.

[5] T. Nenning, M. Hofer, M. Hutterer, M. Schrödl, "Setup with two Self-Sensing Magnetic Bearings using Differential 3-Active INFORM", *ISMB14, 14th International Symposium on Magnetic Bearings*, Linz, Austria, August 11-14, 2014

[6] M. Hofer, M. Hutterer, M. Schrödl, "Application of Soft Magnetic Composites (SMCs) in Position-Sensorless Controlled Radial Active Magnetic Bearings", *ISMB15, 15th International Symposium on Magnetic Bearings*, Kitakyushu, Japan, August 3-6, 2016

[7] Y. Gua, J. G. Zhu, "Application of Soft Magnetic Composite Materials in Electrical Machines", *Australian Journal of Electrical and Electronics Engineering*, Volume 3, 2006 – Issue 1

[8] M. Hutterer, M. Schrödl, "Control of Active Magnetic Bearings in Turbomolecular Pumps for Rotors with Low Resonance Frequencies of the Blade Wheel", *Lubricants, Volume 5, Issue 3*, 25 July 2017